



# Fitting Analytical forms of spatial and temporal correlation functions to spacecraft data

A. Shalchi

Department of Physics and Astronomy, University of Manitoba, Winnipeg, Manitoba R3T 2N2, Canada

Correspondence to: A. Shalchi (andream4@yahoo.com)

Received: 21 June 2012 – Revised: 3 September 2012 – Accepted: 10 September 2012 – Published: 5 October 2012

**Abstract.** Spacecraft missions such as Wind and ACE can be used to determine magnetic correlation functions in the solar wind. From such data sets one can obtain spatial and temporal correlations of magnetic fields. Such correlations are fundamental in the theory of magnetic turbulence and are important to describe the statistics of magnetic field lines and the propagation of energetic particles such as cosmic rays. In the present article we compare analytical forms of correlation functions with measurements performed in the solar system. We obtain new values for the correlations length scales and we test our understanding of the turbulence dynamics.

## 1 Introduction

The understanding of turbulence is fundamental in plasma and astrophysics. In order to achieve a complete theoretical description of turbulence, one has to know the spatial and temporal structures. However, those are difficult to access experimentally. The understanding of turbulent plasmas is important for describing the propagation and acceleration of energetic particles such as cosmic rays. The spatial correlation functions and correlations lengths have a direct influence on the charged particle diffusion coefficients along and across the mean magnetic field (e.g. Shalchi, 2009). The temporal or Eulerian correlations control the parallel diffusion coefficient of low-energy particles (e.g. Bieber et al., 1994; Shalchi et al., 2006). Temporal and spatial correlation functions are also important in the theory of random walking magnetic field lines (e.g. Shalchi et al., 2007, 2012).

In recent years more and more experiments have been performed to study magnetic fields in the interplanetary space. The Advanced Composition Explorer (ACE), for instance, is a space exploration mission to study the solar wind and energetic particles such as galactic cosmic rays. Another example is the WIND satellite which was built to study the solar wind plasma. Cluster II is a space mission of the European

Space Agency to study the Earth's magnetosphere over the course of an entire solar cycle. Simultaneous magnetic field data from Wind, ACE, and Cluster spacecraft can be used to determine the magnetic correlations near Earth's orbit (e.g. Matthaeus et al., 2005; Dasso et al., 2007). Matthaeus et al. (2010) obtained temporal correlations of magnetic fluctuations in the interplanetary field by using Wind and ACE. From such observations detailed information about the spatial and temporal decorrelation of turbulence can be deduced.

The evolution of the interplanetary magnetic field spatial structure has been investigated in the recent years (see Dasso et al., 2005; Ruiz et al., 2011). It was shown that the nature of the turbulence anisotropy differs in the fast ( $V_{SW} > 500$  km/s) and slow solar wind ( $V_{SW} < 400$  km/s). In particular, the fast streams are more dominated by fluctuations with wavevectors quasi-parallel to the local field. Such fluctuations are usually called slab modes. Slow streams, which appear to be more fully evolved turbulence, are more dominated by quasi-perpendicular fluctuation wavevectors. Such fluctuations are usually called two-dimensional modes.

There is also some theoretical work available which allows to compute the correlation functions analytically. Such calculations are based on standard models for interplanetary turbulence (e.g. Matthaeus et al., 2007; Shalchi and Weinhorst, 2009) in the wavevector or Fourier space. It is the purpose of the present paper to compare such analytical forms directly with the measurements performed in the past. This will help to test our understanding of interplanetary turbulence and to obtain turbulence parameters such as the correlation lengths and times.

## 2 Spatial and temporal structure of turbulence

Here we discuss some fundamental quantities which are used to describe magnetic turbulence. More details can be found

in the literature (e.g. Batchelor, 1970; Matthaeus and Smith, 1981; Matthaeus and Goldstein, 1982; Shalchi, 2009).

## 2.1 The turbulence correlation function

A key function in turbulence theory is the two-point-two-time correlation tensor. For homogeneous turbulence its components are

$$R_{lm}(\mathbf{x}, t) = \langle \delta B_l(\mathbf{x}, t) \delta B_m^*(\mathbf{0}, 0) \rangle. \quad (1)$$

The brackets  $\langle \dots \rangle$  used here denote the ensemble average. It is convenient to introduce the correlation tensor in the wavevector space. By using the Fourier representation

$$\delta B_l(\mathbf{x}, t) = \int d^3k \delta B_l(\mathbf{k}, t) e^{i\mathbf{k}\cdot\mathbf{x}} \quad (2)$$

we find

$$R_{lm}(\mathbf{x}, t) = \int d^3k \int d^3k' \langle \delta B_l(\mathbf{k}, t) \delta B_m^*(\mathbf{k}', 0) \rangle e^{i\mathbf{k}\cdot\mathbf{x}}. \quad (3)$$

For homogeneous turbulence we have  $\langle \delta B_l(\mathbf{k}, t) \delta B_m^*(\mathbf{k}', 0) \rangle = P_{lm}(\mathbf{k}, t) \delta(\mathbf{k} - \mathbf{k}')$  with the correlation tensor in the  $\mathbf{k}$ -space  $P_{lm}(\mathbf{k}, t)$ . By assuming the same temporal behavior of all tensor components, we have  $P_{lm}(\mathbf{k}, t) = P_{lm}(\mathbf{k}) \Gamma(\mathbf{k}, t)$  with the dynamical correlation function  $\Gamma(\mathbf{k}, t)$ . Equation (3) becomes then

$$R_{lm}(\mathbf{x}, t) = \int d^3k P_{lm}(\mathbf{k}) \Gamma(\mathbf{k}, t) e^{i\mathbf{k}\cdot\mathbf{x}} \quad (4)$$

with the magnetostatic tensor  $P_{lm}(\mathbf{k}) = \langle \delta B_l(\mathbf{k}) \delta B_m^*(\mathbf{k}) \rangle$ .

## 2.2 The two-component turbulence model

In this paragraph we discuss the static tensor  $P_{lm}(\mathbf{k})$ . Matthaeus and Smith (1981) have shown that for axisymmetric turbulence the correlation tensor has the form

$$P_{lm}(\mathbf{k}) = A(k_{\parallel}, k_{\perp}) \left[ \delta_{lm} - \frac{k_{\parallel} k_m}{k^2} \right], \quad l, m = x, y \quad (5)$$

and  $P_{lz} = P_{zm} = 0$ . In our case the symmetry-axis has to be identified with the axis of the uniform mean magnetic field<sup>1</sup>  $\mathbf{B}_0 = B_0 \mathbf{e}_z$ . Furthermore, we neglect magnetic helicity and we assume that the parallel component of the turbulent field is zero or negligible small ( $\delta B_z \approx 0$ ). A simple model for the function  $A(k_{\parallel}, k_{\perp})$  is the so-called slab model in which we assume the form

$$A^{\text{slab}}(k_{\parallel}, k_{\perp}) = g^{\text{slab}}(k_{\parallel}) \frac{\delta(k_{\perp})}{k_{\perp}}. \quad (6)$$

<sup>1</sup>In most of the physical scenarios,  $\mathbf{B}_0$  is not a real constant and we don't have a uniform field. However, it can be locally defined from an average over spatial scales of the order of the so-called integral scale (see Matthaeus et al., 2012).

Here we have used the Dirac delta function  $\delta(z)$  and the one-dimensional spectrum of the slab modes  $g^{\text{slab}}(k_{\parallel})$  which is discussed below. In this model the wave vectors are aligned parallel to the mean field ( $\mathbf{k} \parallel \mathbf{B}_0$ ).

Another model with reduced dimensionality is the two-dimensional (2D) model where  $A(k_{\parallel}, k_{\perp})$  has the form

$$A^{2D}(k_{\parallel}, k_{\perp}) = g^{2D}(k_{\perp}) \frac{\delta(k_{\parallel})}{k_{\perp}} \quad (7)$$

with the spectrum of the two-dimensional modes  $g^{2D}(k_{\perp})$ . In this model the wave vectors are aligned perpendicular to the mean field ( $\mathbf{k} \perp \mathbf{B}_0$ ) and are therefore in a two-dimensional plane.

In reality the turbulent fields can depend on all three coordinates of space. A more realistic, quasi three-dimensional model for the turbulence is the slab/2D composite (or two-component) model. In the latter model we assume a superposition of slab and two-dimensional fluctuations  $P_{lm}^{\text{comp}}(\mathbf{k}) = P_{lm}^{\text{slab}}(\mathbf{k}) + P_{lm}^{2D}(\mathbf{k})$ . In the composite model the total strength of the fluctuations is  $\delta B^2 = \delta B_{\text{slab}}^2 + \delta B_{2D}^2$ . The composite model is often used to approximate solar wind turbulence. It was demonstrated by several authors (e.g. Bieber et al., 1994, 1996) that the slab fraction should be 20% and the fraction of the two-dimensional modes should be 80%. Therefore the two-dimensional modes should be dominant in the solar wind at 1 AU heliocentric distance.

More turbulence models can be found in the literature. Recently Weinhorst and Shalchi (2010) have extended the slab/2D model to allow a spread of the wave vectors. We expect to find different turbulence properties at different locations. E.g. solar wind turbulence should be different from the interstellar turbulence due to the different driving processes. Some discussions of the different behavior of turbulence in the different physical systems was presented recently (e.g. Hunana and Zank, 2010; Shalchi et al., 2010). In the present article we focus on interplanetary turbulence at short heliocentric distances. In this case the model of slab and two-dimensional modes should provide a good approximation and is in agreement with the observed Maltese cross structure in the solar wind (see Matthaeus et al., 1990; Weinhorst and Shalchi, 2010).

## 2.3 The turbulence spectra

The wave spectrum describes the wave number dependence of  $A(k_{\parallel}, k_{\perp})$ . In the slab model the spectrum is described by the function  $g^{\text{slab}}(k_{\parallel})$  and in the two-dimensional model by  $g^{2D}(k_{\perp})$ . For the two spectra we use the models proposed by Shalchi and Weinhorst (2009)

$$g^{\text{slab}}(k_{\parallel}) = \frac{D(s, q_{\text{slab}})}{2\pi} \delta B_{\text{slab}}^2 I_{\text{slab}} \times \frac{(k_{\parallel} I_{\text{slab}})^{q_{\text{slab}}}}{[1 + (k_{\parallel} I_{\text{slab}})^2]^{(s+q_{\text{slab}})/2}} \quad (8)$$

and

$$g^{2D}(k_{\perp}) = \frac{2D(s, q_{2D})}{\pi} \delta B_{2D}^2 l_{2D} \times \frac{(k_{\perp} l_{2D})^{q_{2D}}}{[1 + (k_{\perp} l_{2D})^2]^{(s+q_{2D})/2}}. \quad (9)$$

Here we have used the turbulence strength of the slab modes  $\delta B_{\text{slab}}^2$  and the 2D modes  $\delta B_{2D}^2$ , respectively. The parameters  $l_{\text{slab}}$  and  $l_{2D}$  are the two bendover scales denoting the turnover from the energy range to the inertial range of the spectrum. In the two model spectra defined above we allow different values of the energy range spectral indexes  $q_{\text{slab}}$  and  $q_{2D}$ . For the inertial range spectral index  $s$  we assume the same values. Furthermore, we used the normalization function  $D(s, q) = \{\Gamma[(s+q)/2]\}/\{2\Gamma[(s-1)/2]\Gamma[(q+1)/2]\}$  where we have used the Gamma function  $\Gamma(z)$ .

## 2.4 Correlation functions for dynamical turbulence

The correlation function for dynamical turbulence is given by Eq. (1) and can be computed by evaluating Eq. (4). Based on the latter formula, Shalchi (2008b) has shown that the combined correlation function  $R_{\perp} = R_{xx} + R_{yy}$  is given by

$$R_{\perp}^{\text{slab}}(z, t) = 8\pi \int_0^{\infty} dk_{\parallel} g^{\text{slab}}(k_{\parallel}) \cos(k_{\parallel} z) \Gamma^{\text{slab}}(k_{\parallel}, t) \quad (10)$$

for slab turbulence and

$$R_{\perp}^{2D}(\rho, t) = 2\pi \int_0^{\infty} dk_{\perp} g^{2D}(k_{\perp}) J_0(k_{\perp} \rho) \Gamma^{2D}(k_{\perp}, t) \quad (11)$$

for two-dimensional turbulence. Here we have used the Bessel function  $J_0(x)$ . The two correlations depend on time  $t$ , the parallel distance  $z$ , and the perpendicular distance  $\rho = \sqrt{x^2 + y^2}$ . To evaluate these equations we have to specify the dynamical correlation functions  $\Gamma^{\text{slab}}(k_{\parallel}, t)$  and  $\Gamma^{2D}(k_{\perp}, t)$  which is done in Sect. 2.6.

## 2.5 Spatial correlation functions

Spatial correlations can be calculated by setting  $t = 0$  in Eqs. (10) and (11). We find for slab modes

$$R_{\perp}^{\text{slab}}(z) = 8\pi \int_0^{\infty} dk_{\parallel} g^{\text{slab}}(k_{\parallel}) \cos(k_{\parallel} z) \quad (12)$$

and for two dimensional modes

$$R_{\perp}^{2D}(\rho) = 2\pi \int_0^{\infty} dk_{\perp} g^{2D}(k_{\perp}) J_0(k_{\perp} \rho). \quad (13)$$

Those functions have been calculated analytically in Shalchi (2008a) for the special case  $q_{\text{slab}} = q_{2D} = 0$ . Here we discuss spatial correlations for the more general spectra defined above. In this case Eq. (12) becomes for slab modes

$$R_{\perp}^{\text{slab}}(z) = 4D(s, q_{\text{slab}}) \delta B_{\text{slab}}^2 \times \int_0^{\infty} dx \frac{x^{q_{\text{slab}}}}{[1+x^2]^{(s+q_{\text{slab}})/2}} \cos\left(\frac{xz}{l_{\text{slab}}}\right) \quad (14)$$

and for two dimensional modes

$$R_{\perp}^{2D}(\rho) = 4D(s, q_{2D}) \delta B_{2D}^2 \times \int_0^{\infty} dx \frac{x^{q_{2D}}}{[1+x^2]^{(s+q_{2D})/2}} J_0\left(\frac{x\rho}{l_{2D}}\right). \quad (15)$$

Here we have used the integral transformations  $x = k_{\parallel} l_{\text{slab}}$  and  $x = k_{\perp} l_{2D}$ , respectively. In Sect. 3.1 we compare these formulas with solar wind data.

## 2.6 An advanced dynamical turbulence model

In order to compute temporal correlations one has to specify the dynamical correlation function  $\Gamma(\mathbf{k}, t)$ . An advanced model for the latter function has been proposed by Shalchi et al. (2006). This model is called the Nonlinear Anisotropic Dynamical Turbulence (NADT) model and is based on an improved understanding of solar wind turbulence (e.g. Shebalin, 1983; Matthaeus et al., 1990; Tu and Marsch, 1993; Oughton et al., 1994; Goldreich and Sridhar, 1995; Zhou et al., 2004; Oughton et al., 2006). To avoid lengthy discussions of this model, we just refer to Shalchi et al. (2006) where this model has been introduced. An important feature of this model is that slab modes and two-dimensional modes are assumed to be coupled, i.e., the slab correlation function  $\Gamma^{\text{slab}}(k_{\parallel}, t)$  can depend on properties of the two-dimensional modes and the dynamical correlation function  $\Gamma^{2D}(k_{\perp}, t)$  can depend on the properties of the slab modes.

As described in Shalchi et al. (2006) and Shalchi (2008b) a reasonable approximation for the two dynamical correlation functions should be given by

$$\Gamma^{\text{slab}}(k_{\parallel}, t) = \cos(\omega t) e^{-\beta t} \quad (16)$$

and

$$\Gamma^{2D}(k_{\perp}, t) = e^{-\gamma(k_{\perp}) t}. \quad (17)$$

Here we have used

$$\gamma(k_{\perp}) = \beta \begin{cases} 1 & \text{for } k_{\perp} l_{2D} \leq 1 \\ (k_{\perp} l_{2D})^{2/3} & \text{for } k_{\perp} l_{2D} \geq 1 \end{cases} \quad (18)$$

which can be approximated by

$$\gamma(k_{\perp}) \approx \beta (1 + k_{\perp} l_{2D})^{2/3} \approx \beta [1 + (k_{\perp} l_{2D})^2]^{1/3} \quad (19)$$

for simplicity. Furthermore, we have employed

$$\beta = \sqrt{2} \frac{v_A}{l_{2D}} \frac{\delta B_{2D}}{B_0}. \quad (20)$$

For the plasma wave dispersion relation we assume parallel propagating shear Alfvén waves with  $\omega = v_A k_{\parallel}$  in Eq. (16).

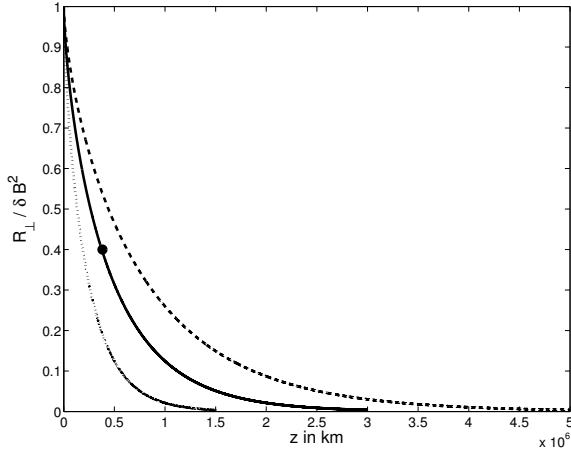


**Fig. 1.** Spatial correlations for slab modes and  $q_{\text{slab}} = 0$ . We compare theoretical results for  $l_{\text{slab}} = 0.3 \cdot 10^6$  km (dotted line),  $l_{\text{slab}} = 0.6 \cdot 10^6$  km (solid line), and  $l_{\text{slab}} = 1.0 \cdot 10^6$  km (dashed line) with the observations (black dot) from Dasso et al. (2007).

**Table 1.** The results for the two-dimensional bendover scale  $l_{2D}$  obtained for different values of the energy range spectral index  $q_{2D}$ . The results were obtained by comparing theoretical results with the observations presented in Dasso et al. (2007).

Spectral index $q_{2D}$	Best fit $l_{2D}$ in km	Best fit $l_{2D}$ in AU
0.0	$0.8 \cdot 10^6$ km	0.005 AU
1.5	$1.7 \cdot 10^6$ km	0.011 AU
5.0	$3.0 \cdot 10^6$ km	0.020 AU

## 2.7 Temporal correlation functions

In the following we calculate the (combined) single-point-two-time correlation function defined by  $E_{\perp}(t) := R_{\perp}(\mathbf{x} = 0, t)$ . The latter function is also known as Eulerian correlation function. We obtain the Eulerian correlations from Eqs. (10) and (11) by setting  $z = 0$  and  $\rho = 0$  therein

$$\begin{aligned} E_{\perp}^{\text{slab}}(t) &= 8\pi \int_0^{\infty} dk_{\parallel} g^{\text{slab}}(k_{\parallel}) \Gamma^{\text{slab}}(k_{\parallel}, t) \\ E_{\perp}^{2D}(t) &= 2\pi \int_0^{\infty} dk_{\perp} g^{2D}(k_{\perp}) \Gamma^{2D}(k_{\perp}, t). \end{aligned} \quad (21)$$

Such correlation functions were already calculated analytically in Shalchi (2008b) for a constant spectrum in the energy range ( $q_{\text{slab}} = q_{2D} = 0$  in our notation). It is straightforward to extend those results for the spectra defined in Eqs. (8) and (9). In this case and for the NADT model the following analytical forms can be found

$$\begin{aligned} E_{\perp}^{\text{slab}}(t) &= 4D(s, q_{\text{slab}}) \delta B_{\text{slab}}^2 \int_0^{\infty} dx \frac{x^{q_{\text{slab}}}}{(1+x^2)^{(s+q_{\text{slab}})/2}} \\ &\times \cos(xv_{At}/l_{\text{slab}}) e^{-\xi v_{At}/l_{2D}} \end{aligned} \quad (22)$$

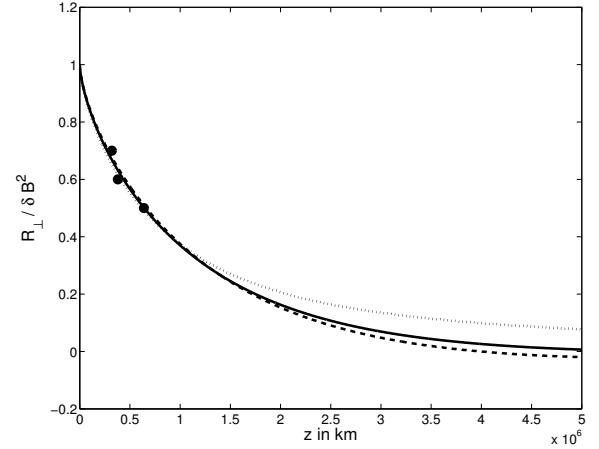


**Fig. 2.** Spatial correlations for two-dimensional modes for different values of  $q_{2D}$ . We compare theoretical results for  $q_{2D} = 0$  with  $l_{2D} = 0.8 \cdot 10^6$  km (dotted line),  $q_{2D} = 1.5$  with  $l_{2D} = 1.7 \cdot 10^6$  km (solid line), and  $q_{2D} = 5.0$  with  $l_{2D} = 3.0 \cdot 10^6$  km (dashed line) with the observations (black dots) from Dasso et al. (2007).

and

$$\begin{aligned} E_{\perp}^{2D}(t) &= 4D(s, q_{2D}) \delta B_{2D}^2 \int_0^{\infty} dx \frac{x^{q_{2D}}}{(1+x^2)^{(s+q_{2D})/2}} \\ &\times e^{-\xi(1+x^2)^{1/3} v_{At}/l_{2D}}. \end{aligned} \quad (23)$$

Here we have used again the integral transformations  $x = k_{\parallel} l_{\text{slab}}$  and  $x = k_{\perp} l_{2D}$ , respectively. Furthermore we have used the parameter  $\xi = \sqrt{2} \delta B_{2D} / B_0$ . In Sect. 3.2 we evaluate Eqs. (22) and (23) numerically and compare our findings with spacecraft data.

## 3 Comparison with spacecraft data

### 3.1 Spatial correlation functions

For slab modes we calculate spatial correlations for  $s = 5/3$  and  $q_{\text{slab}} = 0$  and compare the result with the observations obtained by Dasso et al. (2007). These observations were obtained for the fast solar wind<sup>2</sup> ( $V_{SW} > 470$  km/s). Dasso et al. (2007) (see Fig. 2 for the case  $0^\circ$  of their paper) found for the spatial correlations along the mean magnetic field that  $R_{\perp}(z = 380000 \text{ km}) \approx 0.4$  AU. In Fig. 1 we fit Eq. (12) to the observations. We obtain the best fit for  $l_{\text{slab}} \approx 0.6 \cdot 10^6$  km =  $0.004$  AU<sup>3</sup>. We like to emphasize that  $l_{\text{slab}}$  is the slab bendover scale and not the correlation length. Furthermore, this fit is only correct if we indeed have  $q_{\text{slab}} = 0$ .

<sup>2</sup>It was shown (for instance in Dasso et al., 2005) that the structure of the correlation function can differ for fast and slow solar wind.

<sup>3</sup>Here we used Astronomical Units (AU) which is approximately  $1 \text{ AU} \approx 150 \cdot 10^6$  km.

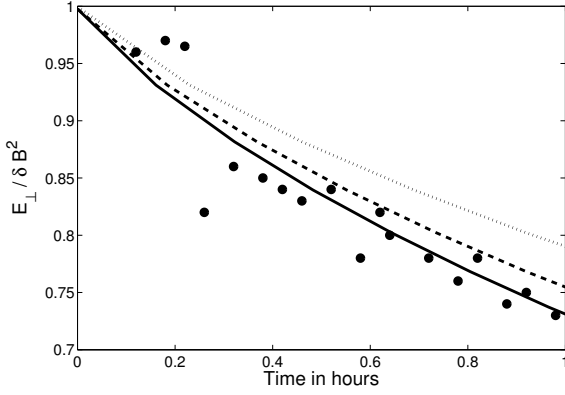


**Fig. 3.** The two-dimensional Eulerian correlation function as a function of the time. The observations (represented by the dots) are from Matthaeus et al. (2010) and the theoretical results were computed by using Eq. (23). For the three theoretical results we assumed that  $\delta B_{2D} = \sqrt{0.8}B_0$ ,  $q_{2D} = 1.5$ ,  $v_A = 12$  km/s, and  $s = 5/3$ . We used different values for the bendover scale of the two-dimensional modes, namely  $l_{2D} = 1.0 \cdot 10^6$  km (dotted line),  $l_{2D} = 0.8 \cdot 10^6$  km (dashed line), and  $l_{2D} = 0.7 \cdot 10^6$  km (solid line).

In Fig. 2 we determine the two-dimensional bendover scale  $l_{2D}$ . In this case it is not clear what the energy range spectral index is (e.g. Matthaeus et al., 2007). Thus, we have calculated spatial correlations for  $s = 5/3$  and for different values of  $q_{2D}$ . For a different energy range spectral index we get the best agreement with the observations for a different bendover scale. Therefore, what we get for  $l_{2D}$  depends on what we assume for  $q_{2D}$ . In Table 1 the different parameter couples are listed. For instance we find the best agreement between theory and observations for  $l_{2D} \approx 1.7 \cdot 10^6$  km corresponding to 0.011 AU if we set  $q_{2D} = 1.5$ .

### 3.2 Temporal correlation functions

Here we compare temporal or Eulerian correlations. As an approximation we assume pure two-dimensional turbulence<sup>4</sup> and set  $\xi = 1.265$ . Furthermore we use again  $s = 5/3$  for the inertial range spectral index and for the Alfvén speed we assume  $v_A = 12$  km/s. In Figs. 3 and 4 we have shown a comparison between the observations (Matthaeus et al., 2010) and the results obtained by evaluating Eq. (23) numerically. We have computed the temporal correlation functions for different values of the two-dimensional bendover scale  $l_{2D}$  and the energy range spectral index  $q_{2D}$ . It should be emphasized that the parameter  $l_{2D}$  is the bendover scale used in Eq. (9) and not the correlation length. As shown in Figs. 3 and 4 we can reproduce the measured temporal correlations. Therefore, we conclude that the observations are consistent with our understanding of the turbulence dynamics.

<sup>4</sup>Here we assume pure two-dimensional turbulence as approximation because two-dimensional modes are dominant in the solar wind (Bieber et al., 1996). In the fast solar wind, however, there is a significant slab contribution.

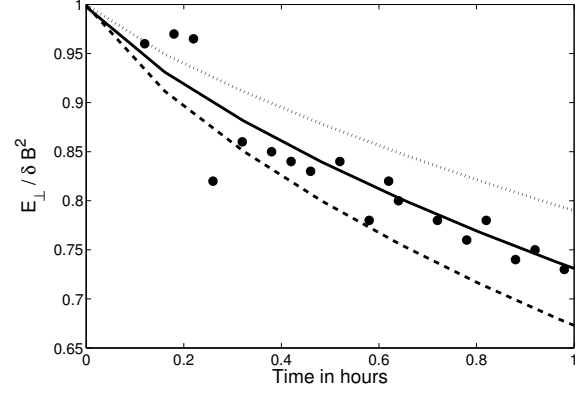


**Fig. 4.** The two-dimensional Eulerian correlation function as a function of the time. The observations (represented by the dots) are from Matthaeus et al. (2010) and the theoretical results were computed by using Eq. (23). For the three theoretical results we assumed that  $\delta B_{2D} = \sqrt{0.8}B_0$ ,  $l_{2D} = 0.7 \cdot 10^6$  km,  $v_A = 12$  km/s, and  $s = 5/3$ . We used different values for the energy range spectral index, namely  $q_{2D} = 0.0$  (dotted line),  $q_{2D} = 1.5$  (solid line), and  $q_{2D} = 5.0$  (dashed line).

## 4 Conclusions

In the present paper we have compared analytical forms for correlation functions based on the work of Shalchi (2008a,b) with spacecraft measurements performed in the solar system for the fast solar wind by using the Advanced Composition Explorer and the Wind spacecraft (e.g. Dasso et al., 2007; Matthaeus et al., 2010). Based on this comparison we found values for the bendover scales of the slab modes and the two-dimensional modes, respectively. For the slab bendover scale we find the best agreement for  $l_{\text{slab}} \approx 0.6 \cdot 10^6$  km = 0.004 AU. For the two-dimensional modes our findings for the bendover scale depends on the assumption of the energy range spectral index  $q_{2D}$  - see Table 1 of the present paper. For  $q_{2D} = 0.0$  for instance we get the best fit by setting  $l_{2D} \approx 0.8 \cdot 10^6$  km = 0.005 AU. For  $q_{2D} = 1.5$ , however, we obtain  $l_{2D} \approx 1.7 \cdot 10^6$  km = 0.011 AU. It seems that the two bendover scales are in the same order of magnitude. The values obtained in the present paper are close to those obtained by Dasso et al. (2007).

We have also compared analytical results for the temporal or Eulerian correlation function with the observations obtained by Matthaeus et al. (2010). In this case we have approximated the turbulence by using two-dimensional modes which are dominant in the solar wind<sup>5</sup> (see Bieber et al., 1996). This comparison is shown in Figs. 3 and 4. As shown the two-dimensional bendover scale  $l_{2D}$  as well as the energy range spectral index  $q_{2D}$  have an influence on the Eulerian correlations. For  $q_{2D} = 1.5$  for instance, we find the best agreement if the bendover scale is  $l_{2D} \approx 0.7 \cdot 10^6$  km

<sup>5</sup>There are indications that there is a significant slab contribution in the fast solar wind.

$= 0.004$  AU. For other values of  $q_{2D}$  we would find the best agreement for a different bendover scale. Obviously the theoretical correlation function for these cases agrees very well with the data points. Our results are summarized in Table 1.

In the current paper we have compared spatial and temporal correlation functions obtained analytically with solar wind observations. By fitting turbulence parameters we obtained a good agreement between theory and observations. We have shown that critical parameters are the bendover scales  $l_{\text{slab}}$  and  $l_{2D}$  as well as the energy range spectral index of the two-dimensional modes  $q_{2D}$ . The results of the current paper show that the observations are consistent with our present understanding of solar wind turbulence which is based on the two-component model.

*Acknowledgement.* A. Shalchi acknowledges support by the Natural Sciences and Engineering Research Council (NSERC) of Canada.

Edited by: T. Laitinen

Reviewed by: two anonymous referees

## References

- Batchelor, G. K.: Theory of Homogeneous Turbulence, Cambridge, 1970.
- Bieber, J. W., Matthaeus, W. H., Smith, C. W., Wanner, W., Kallender, M.-B., and Wibberenz, G.: Proton and electron mean free paths: The Palmer consensus revisited, *Astrophys. J.*, 420, 294, 1994.
- Bieber, J. W., Wanner, W., and Matthaeus, W. H.: Dominant two-dimensional solar wind turbulence with implications for cosmic ray transport, *J. Geophys. Res.*, 101, 2511, 1996.
- Dasso, S., Milano, L. J., Matthaeus, W. H., and Smith, C. W.: Anisotropy in Fast and Slow Solar Wind Fluctuations, *Astrophys. J.*, 635, L181, 2005.
- Dasso, S., Matthaeus, W. H., Weygand, J. M., Chuychai, P., Milano, L. J., Smith, C. W., and Kivelson, M. G.: ACE/Wind multi-spacecraft analysis of the magnetic correlation in the solar wind, *ICRC*, 2007.
- Goldreich, P. and Sridhar, S.: Toward a theory of interstellar turbulence. 2: Strong alfvénic turbulence, *Astrophys. J.*, 438, 763, 1995.
- Hunana, P. and Zank, G. P.: Inhomogeneous Nearly Incompressible Description of Magnetohydrodynamic Turbulence, *Astrophys. J.*, 718, 148, 2010.
- Matthaeus, W. H. and Smith, C.: Structure of correlation tensors in homogeneous anisotropic turbulence, *Phys. Rev. A - General Physics*, 24, 2135, 1981.
- Matthaeus, W. H. and Goldstein, M. L.: Stationarity of magnetohydrodynamic fluctuations in the solar wind, *J. Geophys. Res.*, 87, 10347, 1982.
- Matthaeus, W. H., Goldstein, M. L., and Roberts, D. A.: Evidence for the presence of quasi-two-dimensional nearly incompressible fluctuations in the solar wind, *J. Geophys. Res.*, 95, 20673, 1990.
- Matthaeus, W. H., Dasso, S., Weygand, J. M., Milano, L. J., Smith, C. W., and Kivelson, M. G.: Spatial Correlation of Solar-Wind Turbulence from Two-Point Measurements, *Phys. Rev. Lett.*, 95, 23, 2005.
- Matthaeus, W. H., Bieber, J. W., Ruffolo, D., Chuychai, P., and Minnie, J.: Spectral Properties and Length Scales of Two-dimensional Magnetic Field Models, *Astrophys. J.*, 667, 956, 2007.
- Matthaeus, W. H., Dasso, S., Weygand, J. M., Kivelson, M. G., and Osman, K. T.: Eulerian Decorrelation of Fluctuations in the Interplanetary Magnetic Field, *Astrophys. J. Letters*, 721, L10, 2010.
- Matthaeus, W. H., Servidio, S., Dmitruk, P., Carbone, V., Oughton, S., Wan, M., and Osman, K. T.: Local Anisotropy, Higher Order Statistics, and Turbulence Spectra, *Astrophys. J.*, 750, 103, 2012.
- Oughton, S., Priest, E., and Matthaeus, W. H.: The influence of a mean magnetic field on three-dimensional magnetohydrodynamic turbulence, *J. Fluid Mech.*, 280, 95, 1994.
- Oughton, S., Dmitruk, P., and Matthaeus, W. H.: A two-component phenomenology for homogeneous magnetohydrodynamic turbulence, *Physics of Plasmas*, 13, 042306, 2006.
- Ruiz, M. E., Dasso, S., Matthaeus, W. H., Marsch, E., and Weygand, J. M.: Aging of anisotropy of solar wind magnetic fluctuations in the inner heliosphere, *J. Geophys. Res.*, 116, A10102, 2011.
- Shalchi, A., Bieber, J. W., Matthaeus, W. H., and Schlickeiser, R.: Parallel and Perpendicular Transport of Heliospheric Cosmic Rays in an Improved Dynamical Turbulence Model, *Astrophys. J.*, 642, 230, 2006.
- Shalchi, A., Tautz, R. C., and Schlickeiser, R.: Field line wandering and perpendicular scattering of charged particles in Alfvénic slab turbulence, *Astron. Astrophys.*, 475, 415, 2007.
- Shalchi, A.: Analytical forms of correlation functions and length scales of astrophysical turbulence, *Astrophys. Space Science*, 315, 31, 2008a.
- Shalchi, A.: Forms of Eulerian correlation functions in the solar wind, *Astrophys. Space Science*, 318, 149, 2008b.
- Shalchi, A.: Nonlinear Cosmic Ray Diffusion Theories, *Astrophysics and Space Science Library*, Berlin, Springer, 362, 2009.
- Shalchi, A. and Weinhorst, B.: Random walk of magnetic field lines: Subdiffusive, diffusive, and superdiffusive regimes, *Adv. Space Res.*, 43, 1429, 2009.
- Shalchi, A., Büsching, I., Lazarian, A., and Schlickeiser, R.: Perpendicular Diffusion of Cosmic Rays for a Goldreich-Sridhar Spectrum, *Astrophys. J.*, 725, 2117, 2010.
- Shalchi, A., Dosch, A., Le Roux, J. A., Webb, G. M., and Zank, G. P.: Magnetic-field-line random walk in turbulence: A two-point correlation function description, *Phys. Rev. E*, 85, 026411, 2012.
- Shebalin, J. V., Matthaeus, W. H., and Montgomery, D.: Anisotropy in MHD turbulence due to a mean magnetic field, *J. Plasma Phys.*, 29, 525, 1983.
- Tu, C.-Y. and Marsch, E.: A model of solar wind fluctuations with two components - Alfvén waves and convective structures, *J. Geophys. Res.*, 98, 1257, 1993.
- Weinhorst, B. and Shalchi, A.: Reproducing spacecraft measurements of magnetic correlations in the solar wind, *Month. Not. Roy. Astronom. Soc.*, 403, 287, 2010.
- Zhou, Y., Matthaeus, W. H., and Dmitruk, P.: Colloquium: Magnetohydrodynamic turbulence and time scales in astrophysical and space plasmas, *Rev. Mod. Phys.*, 76, 1015, 2004.